How different is similar – exploring development of Ceropegia sandersonii pitfall flowers to elucidate convergent evolution of floral synorganization

Annemarie Heiduk
University of KwaZulu-Natal School of Life Sciences https://orcid.org/0000-0002-7857-6646
Dewi Pramanik
Naturalis Biodiversity Center
Marlies Spaans
University of Applied Sciences Leiden
Loes Gast
University of Applied Sciences Leiden
Nemi Dorst
University of Applied Sciences Leiden
Monique Welten
Naturalis Biodiversity Center
Barbara Gravendeel (barbara.gravendeel@naturalis.nl)
https://orcid.org/0000-0002-6508-0895

Research

Keywords: Ceropegia, MADS-box genes, RT-PCR, vascularization, micro-CT scanning, SEM, transcriptomics

Posted Date: May 20th, 2020

DOI: https://doi.org/10.21203/rs.3.rs-26955/v1

Version of Record: A version of this preprint was published on December 14th, 2020. See the published version at https://doi.org/10.3390/plants9121767.

Abstract

Background: Lantern plants from the genus *Ceropegia* (Apocynaceae-Asclepiadoideae) have radially symmetric pitfall flowers that are an outstanding example of functional floral complexity with high synorganization of specialized organs. The evolutionary origin and development of these complex flowers is unclear, and the genetic background of floral organ formation is unknown. Flowers with similar deceptive pollination strategies and floral traits convergently evolved in non-related plant lineages. The partially bilaterally flattened trap flowers of pipevines are functionally similar to *Ceropegia* pitfall flowers; many orchid taxa evolved complex fully bilaterally flattened flowers with specialized organs to trap pollinators. This study is the first to investigate the genetic background of pitfall flower development in *Ceropegia*, and to explore (i) convergent evolution of extremely synorganized and complex flowers as well as (ii) the homology of a highly specialized floral organ, the gynostegial corona.

Methods: We obtained transcriptomes from *C. sandersonii* early floral buds and mature sepals, petals, and gynostegia, and analyzed differential expression of selected MADS-box genes in buds and mature floral organs using RT-PCR. In addition, we studied floral ontogeny and vascularization using SEM and 3D X-ray micro-CT scanning.

Results: We identified ten phases of floral development from primordia to mature flowers, and for the first time visualized the vascular system of mature *Ceropegia* pitfall flowers in a 3D-model. We identified 14 MADS-box gene homologs, representing all major MADS-box gene classes, in the floral transcriptomes of *Ceropegia*. Vascular bundle patterns, as revealed by 3D X-ray micro-CT scanning, in combination with high expression of *GLOBOSA* and *AGAMOUS* indicate a staminoid origin of this highly specialized floral organ which starts developing from stage seven onwards. Interestingly, *AGAMOUS-LIKE6* was neither expressed in early floral buds nor in any mature floral organ, in line with the radial symmetry of all *Ceropegia* floral organs.

Conclusion: We detected differential expression of MADS-box genes involved in *Ceropegia* floral organ identity and propose a new ABCDE-model for parachute flowers. We compare this with current models of unrelated plants with similar floral traits but (partially) bilaterally flattened flowers, i.e. *Aristolochia fimbriata* and *Erycina pusilla*. With this comparative approach we lay the foundation for understanding the genetic mechanisms driving convergent evolution of highly specialized deceptive trap flowers.

Background

The origin of flowers was the key to success during angiosperm evolution as it enabled directed pollen transfer to conspecific flowers via animals as pollen vectors and thus, higher reproductive assurance. Flowering plants are now the dominant plants on earth with a breathtaking diversity in floral forms and functions. Flowers are complex entities comprised of typically only four organs, i.e., sepals, petals, stamens, and carpels. However, variability in the number, form, function and arrangement of these organs allowed for immense diversification during the past ~130 million years. In higher angiosperms, organs

are arranged in different floral whorls and their number is reduced and less variable as compared with primitive Magnoliidae (1). The reduction of whorls is the basis for the evolution of fusion and/or mechanical linkage of separate floral organs (synorganization), and thereby further floral complexity (2).

Among the ten largest plant families, the milkweeds (Apocynaceae) are remarkably with regard to diversity in growth form, flower morphology, and pollination strategies (3). Especially species in the subfamily Asclepiadoideae show extreme floral complexity and diversity in pollinator usage (3); their flowers are most complex with high levels of synorganization (1), which is comparable to what is known from orchids (Orchidaceae; 4). Because of their similar levels of floral synorganization, Asclepiadoideae are sometimes referred to as “dicotyledon orchids” (2). In contrast to orchids, which have trimerous flowers, the flowers of Asclepiadoideae are pentamerous, and male and female reproductive organs are fused into a highly specialized organ called the gynostegium. This organ is radially symmetric, as opposed to the zygomorphic orchid gynostemium, but both are involved in pollination. This floral complexity aroused interest of botanists decades ago; thus, structure and ontogenetic development is relatively well known for these flowers (1, 5–8). Most sophisticated among them are the pitfall flowers of the genus *Ceropegia,* commonly known as lantern flowers. These flowers are structurally very complicated with highly functional floral organs elaborately fused to achieve pollination success and reproductive isolation. *Ceropegia* pitfall flowers develop by con- and postgenital fusion of five petals which form a tripartite tubular corolla (see 1). The corolla lobe tips become often apically fused to form a cage-like structure which in *Ceropegia sandersonii,* commonly known as the parachute plant, resembles a parachute (see 9). The flower tip has five orifices through which insects can enter. It further comprises osmophoric tissue as well as slippery surfaces promoting the trapping of pollinators. In many species the flower tip is decorated with movable hairs likely to support fly attraction (see 10). The cylindrical flower tube with slippery surfaces and downward-pointing hairs on the inside make insects fall to be temporarily trapped inside the basal corolla inflation that encloses the gynostegium (see 10). In addition to various devices to catch, temporarily trap and finally release pollinators (10, 11), the ultimate floral complexity is highlighted by pollen transfer via pollinaria, i.e. discrete pollen packages, which are mechanically clipped to the mouthparts of specific flies. Successful pollination requires insertion of a pollinium (clipped to a fly in a donor flower), into one of the five lateral guide rails on the gynostegium of a receptive flower. For functioning of this elaborate pollinator trap, each floral organ had to evolve into a very specific shape at a very particular position (2). The highly synorganized *Ceropegia* flower and the functionality of its floral organs, singly and joint, aroused the interest of naturalists more than a century ago (12, 13). The most detailed and passionate descriptions of floral structure, functional floral parts and tissues, and their complex interaction with flies to achieve pollination were published by Vogel (9, 10, 14, 15). Only recently, studies on chemical ecology of *Ceropegia* species (16–20) elucidated fascinating chemical mimicry strategies such as kleptomyiophily, i.e. mimicry of injured or dead insects as specific food items of kleptoparasitic flies. Apparently, floral chemistry is the key for pollinator attraction in *Ceropegia,* while floral morphology is crucial for successful pollination. However, the molecular genetic processes controlling floral development of *Ceropegia* flowers have not yet been studied and genes which are involved in the formation of specific floral organs are unknown.

Additional novel organs, positioned between the floral whorls of petals and of stamens such as coronas/stelidia (involved in pollination), and pollinia (discrete pollen packages or clustered pollen) convergently evolved in Apocynaceae (Gentianales) and Orchidaceae (Asparagales). Furthermore, pollinator trap flowers and gynostegia/gynostemia (fusion of male and female reproductive organs) evolved in a third unrelated plant family, pipevines (Aristolochiaceae, Piperales). The mechanisms and strategies to trap fly pollinators also show similarities and are extremely divers within these three unrelated plant families. Many deceptive Orchidaceae attract their fly pollinators through sexual or other chemical mimicry, and trap them with the help of cavern-like or motile labellum structures (e.g. *Cypripedium,* 21; *Pterostylis,* 22). In Aristolochiaceae, *Aristolochia* fly pollinators are attracted by food source or oviposition site mimicry (23) and trapped in pitfall flowers functionally comparable to *Ceropegia* flowers, though the perianth in *Aristolochia* is sepal rather than petal derived (see 24). Such similarities in outstanding floral characters in three non-related plant families spread throughout the Angiosperms call for a comparative developmental study to reveal (dis)similarities in floral organ development and perianth identity.

In *Aristolochia,* genes involved in floral development and organ identity are continuously better understood (25–27), and in orchids, deceptive species such as *Phalaenopsis equestris* and *Erycina pusilla* are well studied with regard to the genetic background of floral development (28–34). Here we present the first data on MADS-box gene expression during development of radially symmetric pitfall flowers of *Ceropegia sandersonii,* the parachute plant; it is the first floral transcriptome analyses for *Ceropegia* in general. We identified MADS-box genes expressed in early floral buds and mature flowers, and carved out expression differences between early and late floral stages, as well as between different floral organs. To further explore the evolutionary origin of selected floral organs in *Ceropegia,* we visualized the vascular system of flowers using 3D X-ray micro-computer tomography (micro-CT). Scanning electron microscopy (SEM) was applied to recognize distinct phases during corolla and gynostegium development. We compared our findings to what is known from bilaterally flattened deceptive orchids (*E. pusilla,* 33) and pipevines (*A. fimbriata,* 26, 27) to (i) explore convergent evolution of complex flowers with extreme synorganization and (ii) investigate the homology of the highly specialized corona.

Results

Early bud and gynostegium development

We roughly defined ten phases during floral development of *C. sandersonii* with distinct changes in organ unfolding. Phase one (P1, Figure 1A) is the emergence of a floral primordium adaxially positioned to a floral bract. Phase two (P2, Figure 1B) is defined by initiation of the five sepal primordia. The third phase (P3, Figure 1C) defines corolla initiation with five petal primordia emerging in alternation to the sepals, and in penta-symmetrical order around the developing pollination apparatus. In phase four (P4, Figure 1D+E) the five stamens initiate around the style head. In phase five (P5, Figure 1F+G) the petals completely enclose the developing gynostegium with congenitally fused petal bases and postgenitally

fused petal tips. In this level the stamens are clearly fused and the carpels are still separated. Colleters (glandular outgrowths of the sepals), start to develop as well in this phase. In phase six (P6, Figure 1H-J) the corolla is cylindrical and mainly formed by the postgenitally fused petal tips. Early stage flickering bodies are present on the edges of the petal tips and the “uvula” (see 9) is initiating. Stamens and style head are not yet postgenitally fused; the style head is still di-symmetric as both carpels are still distinct; colleters are prominent. In phase seven (P7, Figure 1K) the corona emerges, the guide rails become formed by anther wings, and corpuscula (parts of the pollinaria) are becoming visible. The carpels are postgenitally united and the style head has a pentagonal shape. In phase eight (P8, Figure 1N) the corona completely surrounds the gynostegium and is fused with the anthers; the nectar cavities are formed underneath the guide rails, and the corona lobe tips start to outgrow the style head. The corona outer surface becomes covered by long trichomes. In phase nine (P9, Figure 1O) the pollinia are formed and two pollinia from neighboring anthers become connected to the corpusculum to form a pollinarium; the corona lobe tips are at least as long as the gynostegium height. In the final phase (P10, Figure 1P), the anthers back off, the pollen sacs release the pollinia, and the translator is hardened. Thus, gynostegium and pollinaria are fully developed, and the flower is mature.

Vascularization in mature flowers

Vascular bundles were studied in three fully mature flowers of *Ceropegia sandersonii* using micro-CT scanning. In the pedicel (Figure 2A, cross section 1), a vascular cylinder of ten (two times five alternating) bundles could be discerned. One set of five bundles forms the sepal supply (Figure 2A+B, green) with one each becoming a sepal midrib bundle. The second alternating set of five bundles (Figure 2A+B, grey) differentiates into the supply for petals (Figure 2A+B, red), stamens (Figure 2A+B, yellow), and carpels (Figure 2A+B, purple). Each bundle of this second bundle set splits into three traces forming a ring of 15 bundles, grouped into five triplets alternating with the sepal midrib bundles (Figure 2A, cross section 2). The middle bundle of each triplet forms the main petal supply (Figure 2A, cross sections 3), while each lateral trace of a triplet fuses with the according lateral trace from the neighboring triplet (Figure 2A, arrows in cross section 2) to form a stamen bundle and also provide traces running into sepals as secondary sepal bundles (Figure 2A+B, pink). Each of these secondary sepal bundles later splits into two resulting in a total of four secondary bundles per sepal (Figure 2A, cross sections 3–5). Thus, each stamen bundle is formed by fusion of two adjacent traces of different origin, and the sepal supply also is of mixed origin. The stamen bundles later split again (Figure 2A, cross section 3) and each provides two thin traces which run into the carpel wall (Figure 2A, cross section 4, purple). These carpel traces further branch resulting in two semicircles with 5–6 bundles each around the carpels. Each carpel is further supplied by a main central bundle (Figure 2A, cross section 5) for which the origin could not be retraced; both these main bundles fuse where the carpel tips are congenitally fused. However, at the tip of the fused carpels the merged carpel bundle seems to run into the style head where it again divides into branching bundles. No vascular traces could be detected in the corona and colleters. A movie of a rotating 3D model of the vascular system in a mature trap flower of *C. sandersonii* can be found in the supplement (Additional file 7).

Differential gene expression—RT-PCR experiments

The expression of six isolated MADS-box gene homologs, i.e. *CsanFUL2, CsanTM6, CsanGLO, CsanAG2, CsanAGL6,* and *CsanSEP1,* was analyzed in early stage floral buds and in sepals, petals, gynostegia, and coronas of mature flowers using semi-quantitative RT-PCR. Overall, these genes showed distinct expression patterns in time and space (Figure 3). *CsanFUL2* was found to be expressed in early floral buds, and in sepals and gynostegia of mature flowers. *CsanTM6* was only found to be active in mature sepals. *CsanGLO* was expressed in all tissue types analysed, *CsanAG2* was active in early floral buds, and mature gynostegia and corona tissue. *CsanSEP1* was expressed in mature petals and gynostegia, whereas *CsanAGL6* was not expressed in any of the tissues analyzed.

Discussion

Our study is the first comprehensive evolutionary developmental analysis of *Ceropegia* pitfall flowers which belong to the most complicated flowers within the Apocynaceae.

Although the basic floral Bauplan is similar in each species, the variety of floral shapes and colors is huge in *Ceropegia.* The Giant *Ceropegia, C. sandersonii,* has eye-catching parachute-like pitfall flowers that are highly popular as ornamental plant. Besides being among the most charismatic and well-known *Ceropegia* species, it is also the only species thus far for which the pollination strategy has been fully elucidated: with its flower scent it mimics a defending honey bee attacked by a predator and thereby lures scavenger flies as unwilling pollinators (18).

We studied floral development in highly synorganized *Ceropegia sandersonii* pitfall flowerscombining morphological (SEM and micro-CT) and molecular genetic (transcriptomics and RT-PCR) analyses. We, for the first time, visualized and remodeled the vascular system in a *Ceropegia* pitfall flowers. Comparing our results to what is known in other plant groups with similar floral traits and pollination strategies. i.e. Aristolochiaceae and Orchidaceae, provides new insights into the current picture of gene expression during development of specialized floral morphologies. Our comparative approach is a first step to understand convergent evolution of trap flowers that employ highly specialized floral organs (i.e. gynostegia/gynostemia, pollinia and corona/stelidia), and strategies (visual/olfactory deception) to ensure reproductive isolation and associated plant species diversification.

Morphological investigation of flower development

Though several morphological studies on flower development are published for Apocynaceae (e.g. 8, 35, 36), development of *Ceropegia* flowers was never visualized from primordia to fully developed flowers

(but see 2, 10). We used scanning electron microscopy to circumscribe flower development of *Ceropegia sandersonii* from initiation of floral primordia to a mature flower. A SEM image sequence of successive flower development was created, and we could define ten developmental phases (P1-P10, Figure 1A-P) in which clear changes in organ formation take place. This framework lays the foundation for investigating gene expression during each of the defined developmental phases to identify key genes responsible for consecutive changes. Flowers of *C. sandersonii* are special and different from many other species in ways (9). The flower tip forms a parachute-like structure with complex ontogenetic development (but see 9). This special morphology of the flower tip is not unique to *C. sandersonii;* petal tips fused in a parachute-like structure, though less marked than in *C. sandersonii,* is also a feature in a few other species, such as *C. rendallii, C. fimbriata, C. galeata, C. huberi,* and *C. connivens.*

The development of the gynostegial corona only starts its development in phase P7 out of ten phases, which is relatively late. Late appearance of corona tissue has been described in other *Ceropegia* species (5) as well as in other Asclepiadoideae (see 35). The evolution of the gynostegial corona, as determined by previous morphological studies, was described to be of staminoid (androecial) origin for Asclepiadoideae (see 6). Coronas of corolline origin, and consequently with a distinct development, are known from several taxa spread over Apocynaceae (e.g. see 8).

Vascularization of Ceropegia pitfall flowers

Novel 3D X-ray micro-computer tomography techniques (micro-CT) proved to be a powerful tool to study vascularization of orchid flowers (e.g. *Erycina pusilla,* 33, *Phalaenopsis equestris,* 34). To the best of our knowledge this method has not yet been applied to any species in the Gentianales before. Usually, the positions and connections of vascular bundles are studied using microtome slicing and microscopic investigation of selected slices. The description of a vascular system is then based on a few selected slices and sketched sections. The disadvantage of this approach is that the entire vascular system hardly be visualized in its original three-dimensional structure. Studying vascularization with micro-CT provides a more comprehensive and informative insight into the evolutionary origin of different floral organs. The resulting 3-dimensional image of the entire vascular system can be rotated and studied from all possible perspectives to identify the origins of tissue specific vascular bundles. These 3D data facilitate conclusions on the evolutionary origin of floral organs of unclear homologies.

We applied micro-CT scanning to study floral vascularization in mature *Ceropegia sandersonii* pitfall flowers and our data allowed to re-model the vascular system of these complex flowers which gave interesting new insights into how their different floral organs are connected via vascular bundles (Figure 2). Each stamen is supported by a single vascular bundle which runs all the way through this floral organ without branching just as described for other Apocynaceae (37). We found that stamen bundles are formed by fusion of veins with separate origin, i.e. bundles that derive from two neighboring main bundles (Figure 2A, cross section 2; Figure 2B–4). The double origin of stamen bundles was already described and discussed in other plants (38, 39). Also, vascular bundles running into the sepals were

found to be of mixed origin, i.e. one main bundle is joined by secondary bundles branching off from an adjacent bundle (Figure 2B–3). Carpels were found to be supplied by vascular bundles originating from stamen bundles (Figure 2A) which seems a logical consequence of the fusion event of androecium and gynoecium to form the gynostegium as a novel organ. We did not discern vascular bundles in the corona which confirms what was described for other Apocynaceae (37). Coronal structures generally seem to be non-vascular; the only bundles observed were marginal petal or staminal bundles (37). Absence of vascular bundles in the corona of *Ceropegia sandersonii* supports that this organ is an emergence of the stamens. It further suggests that the corona does not produce nectar via coronal nectaries as described for other species of Apocynaceae-Asclepiadoideae (35). The presence of nectar in *C. sandersonii* was never empirically verified. Thus, if present at all, the primary nectaries should be found beneath the guide rails, and the coronal nectar cups around the gynostegium only collect but not produce nectar (see 40). It would be very interesting to further explore whether in other species with coronal nectaries the coronas are not vascularized either.

MADS-box genes driving floral organ identity

We identified differentially expressed MADS-box genes involved in formation of highly synorganized *Ceropegia* pitfall flowers. Based on our results and on what is generally known about MADS-box gene expression in flowering plants (for review see 41), we propose a modified ABCDE model of floral organ identity for *Ceropegia (*Figure 4). According to this model, A-class genes are expressed in mature sepals and gynostegia. B-class genes are expressed in mature sepals, petals, corona, stamens, and the corona but not in the gynoecium (carpels and ovules). C-class genes are expressed in the mature corona, stamens, and carpels but not in the ovaries. D-class genes are only active in ripening ovules, and E-class genes are expressed in all floral organs.

In our *Ceropegia sandersonii* floral transcriptomes we could identify three A-class genes, i.e. two copies of *FRUITFULL* (*FUL)* and one copy of *APETALA1* (*AP1),*, and our expression analyses indicated that A-class genes play a role in formation of mature sepals and gynostegia (see Additional file 6).

B-class genes generally control identity of petals and stamens. In our expression analyses we found that the *GLOBOSA* homolog *CsanGLO* is expressed in all investigated floral organs, which indicates a key function of this B-class gene in development of *Ceropegia* pitfall flowers, in line with the floral quartet model. In the corona, a highly specialized organ situated in the floral whorl positioned between the whorls containing the stamens and corolla, and unique to Apocynaceae, *CsanGLO* was found to be expressed together with the C-class gene *AGAMOUS* (*CsanAG2)*.. This, again, supports the idea that the corona in Asclepiadoideae is of staminal origin. Due to the exceptional diversity of corona morphology and development (petal or/and stamen derived, i.e. corolline or/and staminal) within Apocynaceae, the evolutionary origin and homology of this floral organ is not yet fully understood. Based on previous ontogenetic studies with traditional anatomical methods, the corona was assumed to be corolline in

Rauvolfioideae, Apocynoideae, and Periplocoideae, but typically of staminal origin in Asclepiadoideae and Secamonoideae (6, 8, but see 35). Our results further support this last hypothesis.

In orchids, combined MADS-box B- and C-class gene expression was also found in other highly specialized floral organs of staminodal origin in a floral whorl, situated between the petals and stamens, the stelidia. In the stelidia, however, expression of *AGL6* was also detected, which was not found in the corona of *C. sandersonii.* Whether the presence of expression of *AGL6* in orchid flower stelidia but absence in parachute flower coronas is correlated with the bilateral symmetry of the first and radial symmetry of the latter organ remains to be investigated.

Interestingly, no *AGL6* expression was detected in the early floral buds or any of the mature organs of *C. sandersonii* flowers that are all radially symmetric. This finding is in contrast with previous findings of Pabón-Mora et al. (26), who detected *AGL6* expression in the bilaterally symmetric sepals and ovules of the pipevine *Aristolochia fimbriata* and Dirks-Mulder et al. (33) and Pramanik et al. (34), who detected *AGL6* expression in the bilaterally symmetric sepals, petals, stelidia and gynostemium in the first, second, third and fourth whorl of the flowers of the orchid species *Erycina pusilla, Phaelonopsis equestris* and *P. pulcherrima.*

No E-class gene expression was found in the mature corona of *Ceropegia* sandersonii. In the callus on the orchid labellum, also an organ of staminal identity (33, 34), E-class gene expression was found. Expression was more pronounced in early than late developmental stages of the callus and thus, E-class gene expression may take place in the early stage *Ceropegia* corona as well. This aspect, however, could not be assessed because early stage coronas were too small to dissect for RNA extractions. Laser capture microdissection could be applied to further investigate this.

E-class gene expression in *Ceropegia* was restricted to mature petals and gynostegia. This is different as compared with *Aristolochia* (26, 42) and *Erycina (*33), where E-class gene expression was also found in early stage floral buds, but congruent with the finding for *Coffea (*43), where no E-class gene expression was detected in young floral buds either. The timing of E-class gene expression pattern found seems correlated with the positions of the species investigated in the Tree of Life for the Angiosperms (44): late stage E-class gene expression in Eudicots seems to have evolved from early and late stage expression in Monocots.

E-class gene expression was also detected in the mature gynostemia of *Aristolochia (*26, 42), *Erycina (*33), and *Phalaenopis (*34) and we assume that these similarities are correlated to the fusion of male and female reproductive functions in a single organ.

E-class gene expression in mature petals was also found in *Erycina (*33). In *Aristolochia,* the pitfall flowers are sepaloid and petals are lacking (24).

The MADS-box expression patterns found were summarized in Figure 4 in which we propose a first ABCDE-model for parachute flowers and compare this to previous models constructed for other deceptive

flowers in the orchid and pipevine families.

Conclusion

This study for the first time investigated in comprehensive detail the development of highly complex and synorganized *Ceropegia* pitfall flowers using the parachute plant *C. sandersonii* as model species. We combined micro-morphological (SEM and micro-CT) and molecular techniques (transcriptome and RT-PCR analysis) to unravel floral organ development and identity. In a SEM image series from floral primordia to fully mature flowers we identified ten phases with distinct changes in floral organ development. We furthermore performed the first transcriptome analyses of early buds and different tissues (sepals, petals, corona, gynostegium) of mature *Ceropegia* pitfall flowers and determined MADS-box genes involved in floral organ identity. MADS-box genes expressed in the mature corona, a floral organ unique to Apocynaceae, revealed its staminal origin in *C. sandersonii* (Asclepiadoideae). This is the first time that the origin of the corona was clarified using molecular methods in a species of Apocynaceae. The corona emerges late during floral development and becomes first distinct only in phase seven out of ten. Neither the corona nor any other tissue was found to express *AGL6.* In unrelated plants with similar floral traits but bilaterally flattened flowers, i.e. *Aristolochia fimbriata* and *Erycina pusilla, AGL6* controls symmetry and is also expressed in orchid stelidia, a floral organ likely homolog to the staminal corona in Apocynaceae. Its absence of expression in *Ceropegia* flowers presumably leads to their radial symmetry. Based on our results, we propose an ABCDE model for parachute flowers, and with our comparative approach to non-related plants with similar floral traits we take the first step towards understanding the genetic mechanisms driving convergent evolution of highly specialized deceptive trap flowers.

Materials And Methods

Plant material

Twelve individual plants of *Ceropegia sandersonii,* commonly known as Giant *Ceropegia,* were purchased from Paul Shirley Succulents (https://www.paulshirleysucculents.nl/) and cultivated in the Hortus botanicus Leiden, The Netherlands.

Fixation of flowers for micromorphology (micro-CT, SEM)

Fresh mature flowers and buds were harvested in different stages and fixed with standard formalin-aceto-alcohol (FAA: absolute ethanol, 90%; glacial acetic acid, 5%, formalin; 5% acetic acid). The samples were stored at room temperature until further use.

Scanning electron microscopy (SEM)

Floral buds at different developmental stages were dissected in 70% ethanol and subsequently washed twice each with 70% and 96% ethanol. The material was then transferred to 100% acetone which was changed after 30 min. Subsequently, the samples were critical point dried using liquid CO_2 with a Leica EM CPD300 critical point dryer (Leica Microsystems, Wetzlar, Germany), and mounted on aluminium stubs using either double-sided carbon tape or Leit-C carbon cement. A Quorum Q150TS sputter coater (Quorum Technologies, Laughton, East Sussex, UK) was used to coat the samples with a 20nm thin layer of Platina-Palladium. Imaging of samples was performed with a JEOL JSM–7600 F Field Emission Scanning Electron Microscope (JEOL Ltd., Tokyo, Japan).

3D X-ray micro-computer tomography (micro-CT)

Fresh mature flowers were stained for 5 days with 1% phosphotungstic acid (PTA) in 70% ethanol as contrast agent whereby PTA was change daily. After staining, flowers were washed twice with 70% ethanol and embedded in 1.5% low melting point agarose in a plastic container. Embedded flowers were scanned using a Zeiss Xradia 510 Versa 3D X-ray equipped with a sealed transmission X-ray source (settings: voltage/power: 40 kV/3 W; source current: 75 µA; exposure time: 2 sec; camera binning 2; optical magnification: 4x; pixel size: 3.5 µm; total exposure time: ~3–2 h). Single 2D images were stacked to build a 3D image which was processed using Avizo 3D software version 8.1 (Thermo Scientific™).

RNA isolation

Early floral buds (<3 mm) and mature flowers (first day of anthesis) were harvested from at least three different plant individuals. Mature flowers were dissected to sepals, petals (tip, tube, base), gynostegium, and corona. Similar tissue types of different mature flowers were pooled to reach the required amount of tissue needed for RNA isolation (~30–90 mg). All samples were snap-frozen in liquid nitrogen and stored at –80°C until RNA isolation. Plant tissue was ground in a 2.2 ml micro centrifuge tube with a 7 mm glass bead using TissueLyser II (QIAGEN). Total RNA was extracted using the RNeasy Plant Mini Kit (QIAGEN) and an adapted protocol which included a step to digest single- and double-stranded DNA (DNase I; Amp Grade, Invitrogen 1U/µl). The amount of RNA for RT-PCR was measured using a NanoDrop (ND–1000 Spectrophotometer, Marshall Scientific). Samples used for RNA sequencing were further quality checked by determining the integrity (RNA Integrity Number; RIN) using the Plant RNA nano protocol on an Agilent 2100 Bioanalyzer (Agilent Technologies). Only samples with a RIN >9.5 were used for sequencing. To obtain a full petal sample, RNA extracted separately from petal tips, tubes and bases was pooled after quality control. RNA samples were sent to Beijing Genomics Institute (BGI) for NGS sequencing on an Illumina HiSeq platform.

Transcriptome analyses and MADS-box gene identification

An in-house designed bioinformatics pipeline was used for quality control, assembly, annotation and differential expression analyses. Raw read pairs obtained from NGS sequencing were quality checked using FastQC v0.10.1 (http://www.bioinformatics.babraham.ac.uk/projects/fastqc). Low quality reads were trimmed or removed with Trimmomatic v0.32 (45) and remaining reads were again quality checked. Trinity v2.5.1 (46) was used for *de novo* assembly of cleaned reads, and alignment of reads was performed using Bowtie2 v2–2.3.3.1 (47). CDHIT-EST (48) was used to cluster contigs and to create consensus sequences (unigenes) against which the reads were aligned using RSEM v1.3.0 (49) and Bowtie2 v2–2.3.3.1. Raw counts per read were quantified and a count table was generated with an *in house* designed bioinformatics script (https://github.com/naturalis/orchid-transcriptome-pipeline/tree/master/Scripts).

All *Ceropegia sandersonii* gene sequences were blasted against a local database of Gentianales MADS-box gene homologs (Rubiaceae: *Coffea arabica, Gardenia jasminoides;* Gentianaceae: *Gentiana scabra;* Apocynaceae: *Allamanda cathartica, Catharanthus roseus),*, which was created by retrieving DNA sequences from NCBI GenBank. Sequences for Actin were also retrieved to identify the *C. sandersonii* actin homolog required as control gene for the RT-PCR experiments (see below). For identified *C. sandersonii* MADS-box gene homologs (see Additional file 2), expression differences between sample types and among sample replicates were visualized in a heatmap (based on the count table for the according sequences; Additional file 6) using an *in house* designed bioinformatic script (https://github.com/naturalis/orchid-transcriptome-pipeline/tree/master/Scripts). With this script, the number of matches between a specific read in the transcriptomes and a reference gene was scored. In a separately generated 'Color Key and Histogram', the number of hits was translated to color codes. Color codes were based on the number of counts per gene and sample divided by the total number of counts, where cold colors correspond with a relative low number and war colors with a relative high number. Additional differential expression analyses were carried out using DESeq in R to calculate the log2 fold change of expression of the genes investigated in the different floral organs and developmental phases. Six pairwise tests between the four sample types 'early buds', 'sepals', 'petals', and 'gynostegium' were performed (see Additional file 4). These tests identify those genes with significant differential expression (minimum log2 fold change of 0.25) between a given pair of sample types. All samples had >100 counts so that a cut-off for the analyses was not necessary.

Phylogeny of MADS-box gene lineages

To assess phylogenetic relationships between Gentianales MADS-box gene lineages, all publicly available DNA sequences (see Additional file 3) plus those from the newly identified *Ceropegia sandersonii* homologs (see Additional file 2) were translated to amino acids in the correct translation frame by using translate-protein tools (http://reverse-complement.com/translate-protein/ROOT/), loaded into Geneious Prime® 2019 v.2.3 (www.geneious.com) and aligned with the best matching open reading frame (from start to stop codon) using the 'Geneious alignment' function. The created alignment was trimmed down to the most conserved regions (protein domains and amino acid motifs) to ensure all sequences had

similar length; regions that did not align were removed prior to further analysis. Separate alignments were made for each MADS-box gene subfamily, and combined in a Maximum Likelihood phylogenetic analysis using the PhyML plugin (50) with the following settings: substitution model 'Blosum62'; Bootstrap '100'; proportion of invariable sites '0, fixed'; number of substitution rate categories '4'; gamma distribution parameter '0, estimated'; optimize 'Topology/length/rate'; topology search 'NNI (default, fast)'. As outgroup, sequences which did not fall into the major subfamily clades were chosen, i.e. *SEEDSTICK* sequences of *Gentiana scabra* (*GsSTK1)* and the according homolog of *Ceropegia sandersonii (CsanSTK1)*..

Primer design and cDNA Synthesis

Six MADS-box gene homologs (*CsanFUL2, CsanTM6, CsanGLO, CsanAG2, CsanAGL6, CsanSEP1)* were chosen for further analyses as they showed most divergent expression patterns in the transcriptome analyses. Detailed expression patterns were investigated in early floral buds and mature sepal, petal, gynostegium, and corona tissue. Primers were designed using the online software Primer3Plus (https://primer3plus.com/cgi-bin/dev/primer3plus.cgi) with the following settings: max Poly-X = 3; CG-Clamp = 2; max. End GC = 2). All primer pairs (see Additional file 1) were screened for specificity in a gradient PCR reaction with a reaction mixture (25 µl) containing 10x CoralLoad Buffer (Qiagen), 25mM $MgCl_2$ (Qiagen), 100 mM Bovine Serum Albumin, Acetylated-BSA (Promega), 1.25x DMSO (Qiagen), 5x Q-Solution (Qiagen), 0.2 µM of each primer (IDT), 2.5 mM dNTPs (Qiagen), and 1.25 units/50 µl DNA *Taq* Polymerase (Qiagen), plus 100 ng cDNA template. MQ water (Ultrapure) was used to reach the final volume of 25 µl. The amplification started with an initial denaturation step of 6 min at 94°C, continued with 38 cycles of three steps consisting of 1 min at 94°C, 1 min at 52°C–55°C, and 2 min at 72°C, and was finalized with one amplification step of 12 min at 72°C.

From RNA extracted of early floral buds, and sepals, petals, gynostegia, and corona tissue of mature flowers, cDNA was synthesized using SuperScript III reverse transcriptase (Invitrogen). As a first step the reaction mix containing the RNA template (10 pg–5 µg), 1 µl 10 mM dNTP Mix, 50 µM Oligo $(dT)_{20}$, and sterile distilled water (final volume: 14 µl) was heated at 65C for 5 minutes. After incubation on ice for at least one minute, the mix was briefly centrifuged, then 5X first-stand buffer (4 µl), 0.1 MDTT (1 µl), and 200 units/µL Superscript III (1 µl) were added. This mixture was then incubated at 55C for 50 minutes to dissolve the RNA template while avoiding formation of secondary structures; heating at 70C for 15 minutes inactivated the reaction. A reaction mix without RNA template (non-template control, NTC) was used as negative control. Quantity and quality of cDNA were measured via nanodrop (ND–1000 Spectrophotometer, Marshall Scientific). A total of 90 ng per cDNA sample was then used for PCR-amplification with sequence specific primers (see below). The Actin gene homolog (*CsanACT)* was used as positive control and a non-template reaction DNA (NTC) was used as negative control.

Reverse Transcription PCR (RT-PCR)

Semi-quantitative reverse transcription-PCR (RT-PCR) was performed for six selected MADS-box gene homologs, i.e. *CsanFUL2, CsanTM6, CsanGLO, CsanAG2, CsanAGL6,* and *CsanSEP1.* The thermal cycling regime used in the RT-PCR reaction was similar as for the gradient PCR (see above); however, the annealing temperature was set to 52°C as this temperature yielded the best results and most specific products in the gradient PCR. Actin was amplified as a positive control; the negative control was a non-template control (NTC). All reactions were carried out in a CFX384 Touch Real-Time PCR system thermocycler (Biorad). The PCR products were run on a 1% agarose gel with 1x TAE and a 1 kb plus GeneRuler^{TM} (Thermo Scientific) as ladder. The gel was stained with ethidium bromide and digitally photographed using a gel doc (Ultima 10si, Isogen Life Science).

Abbreviations

AG:AGAMOUS;

AGL6: AGAMOUS-LIKE-6;

AP3: APETALA3;

DEF:DEFICIENS;

FUL: FRUITFULL;

GLO:GLOBOSA;

micro-CT: 3D X-ray micro-computed tomography;

RT-PCR: Reverse transcription polymerase chain reaction;

SEM: Scanning electron microscopy;

SEP: SEPALLATA;

STK: SEEDSTICK;

Declarations

Ethics approval and consent to participate

Not applicable for present study.

Consent for publication

All authors have provided consent for publication.

Availability of data and material

Data supporting the results reported in this article are available as Additional files 1–7 (see above).

Competing interests

The authors declare that the research was conducted in sound collaboration and absence of any non-financial, financial or commercial relationships that could be considered as potential conflicting and/or competing interest.

Funding

This study was supported by a grant from the *Alberta Mennega Foundation* and a *Martin and Temminck fellowship* to AH in 2018 and 2019, respectively.

Author's contribution

The study was conceptualized by AH but supervised and hosted by BG. AH and BG lead the research team during data collection and analyses. Data was collected by AH, DP, and MS. LS and ND performed the bioinformatic analyses of transcriptome data. DP constructed the phylogenetic tree. DP and MS performed the RT-PCR experiments. AH performed SEM image series AH and sample preparation for micro-CT. AH, BG, and MW analyzed 3D X-ray CT-scans of flowers. AH contrived the 3D model of vascularization which was verified and finalized by BG and MW. AH and BG wrote the manuscript and all authors read and approved the final version.

Acknowledgements

We thank Niels Meesters, Rob Langelaan, and Bertie Joan van Heuven for help with laboratory work, Martin Rücklin for help with AVIZO, and Rogier van Vugt (Hortus botanicus Leiden) and especially Paul Shirley for keeping the study plants happy. We furthermore thank Anita Dirks-Mulders for vivid discussions and advice, and Ulrich Meve for valuable comments on the final manuscript draft. We also thank Jürg Schönenberger and Susanne Pamperl (University of Vienna) for performing additional 3D X-ray CT-scans of *Ceropegia sandersonii* flowers.

References

1. Endress PK. Patterns of floral construction in ontogeny and phylogeny. Biol J Linn Soc. 1990;39(2):153-75.

2. Endress PK. Development and evolution of extreme synorganization in angiosperm flowers and diversity: a comparison of Apocynaceae and Orchidaceae. Ann Bot. 2016;117:749-67.
3. Ollerton J, Liede-Schumann S, Endress ME, Meve U, Rech AR, Shuttleworth A, et al. The diversity and evolution of pollination systems in large plant clades: Apocynaceae as a case study. Ann Bot. 2018;123(2):311-25.
4. Rudall PJ, Bateman RM. Roles of synorganisation, zygomorphy and heterotopy in floral evolution: the gynostemium and labellum of orchids and other lilioid monocots. Biol Rev. 2002;77(3):403-41.
5. Hofmann U, Specht AK. Der morphologische Charakter der Asclepiadaceencorona. Beitr Biol Pfl. 1986;61:79-85.
6. Liede S, Kunze H. A descriptive system for corona analysis in Asclepiadaceae and Periplocaceae. Plant Sys Evol. 1993;185(3-4):275-84.
7. Rao V, Ganguli A, editors. The floral anatomy of some Asclepiadaceae. Proceedings of the Indian Academy of Sciences-Section B; 1963: Springer.
8. Kunze H. Morphology and evolution of the corolla and corona in the Apocynaceae s.l. Bot Jahrb. 2005;126(3):347-83.
9. Vogel S. Über die "Uvula" von *Ceropegia sandersonii* Hook. f. - zugleich über einen merkwürdigen Fall postgenitaler Verwachsung. Beitr Biol Pfl. 1960;35(3):395-412.
10. Vogel S. Die Bestäubung der Kesselfallen-Blüten von *Ceropegia*. Beitr Biol Pfl. 1961;36:159-237.
11. Müller L. Zur biologischen Anatomie der Blüte von *Ceropegia woodii* Schlechter. Biol Gen. 1926;2:799-814.
12. Delpino F. Ulteriori osservazioni e considerazioni sulla dicogamia nel regno vegetale. Atti Soc Ital Sci Nat. 1869;1:214-8.
13. Knuth P. Handbuch der Blütenbiologie. Leipzig: Engelmann Verlag; 1898-1905.
14. Vogel S. Blütenbiologische Typen als Elemente der Sippengliederung, dargestellt anhand der Flora Südafrikas: Fischer, Jena; 1954. 338 p.
15. Vogel S. Kesselfallen-Blumen. Umsch Wiss Tech. 1965;65:12-7.
16. Heiduk A, Brake I, Tolasch T, Frank J, Jürgens A, Meve U, et al. Scent chemistry and pollinator attraction in the deceptive trap flowers of *Ceropegia dolichophylla*. S Afr J Bot. 2010;76(4):762-9.
17. Heiduk A, Kong H, Brake I, von Tschirnhaus M, Tolasch T, Tröger A, et al. Deceptive *Ceropegia dolichophylla* fools its kleptoparasitic fly pollinators with exceptional floral scent. Front Ecol Evol. 2015;3(66):doi:10.3389/fevo.2015.00066.
18. Heiduk A, Brake I, von Tschirnhaus M, Göhl M, Jürgens A, Johnson Steven D, et al. *Ceropegia sandersonii* mimics attacked honeybees to attract kleptoparasitic flies for pollination. Curr Biol. 2016;26:2787-93.
19. Heiduk A, Brake I, von Tschirnhaus M, Haenni J-P, Miller R, Hash J, et al. Floral scent and pollinators of *Ceropegia* trap flowers. Flora. 2017;232:169-82.

20. Heiduk A, Haenni J-P, Meve U, Schulz S, Dötterl S. Flower scent of *Ceropegia stenantha*: electrophysiological activity and synthesis of novel components. J Comp Physiol A. 2019;205:301–10.
21. Braunschmid H, Mükisch B, Rupp T, Schäffler I, Zito P, Birtele D, et al. Interpopulation variation in pollinators and floral scent of the lady's-slipper orchid *Cypripedium calceolus* L. Arthropod Plant Interact. 2017;11(3):363-79.
22. Phillips RD, Scaccabarozzi D, Retter BA, Hayes C, Brown GR, Dixon KW, et al. Caught in the act: pollination of sexually deceptive trap-flowers by fungus gnats in *Pterostylis* (Orchidaceae). Ann Bot. 2013;113(4):629-41.
23. Oelschlägel B, Nuss M, von Tschirnhaus M, Pätzold C, Neinhuis C, Dötterl S, et al. The betrayed thief: the extraordinary strategy of *Aristolochia rotunda* to deceive its pollinators. New Phytol. 2015;206(1):342-51.
24. González F, Stevenson DW. Perianth development and systematics of *Aristolochia*. Flora. 2000;195(4):370-91.
25. Jaramillo MA, Kramer EM. *APETALA3* and *PISTILLATA* homologs exhibit novel expression patterns in the unique perianth of *Aristolochia* (Aristolochiaceae). Evol Dev. 2004;6(6):449-58.
26. Pabón-Mora N, Suárez-Baron H, Ambrose BA, González F. Flower development and perianth identity candidate genes in the basal angiosperm *Aristolochia fimbriata* (Piperales: Aristolochiaceae). Front Plant Sci. 2015;6:1095.
27. Peréz-Mesa P, Ortíz-Ramírez CI, González F, Ferrándiz C, Pabón-Mora N. Expression of gynoecium patterning transcription factors in *Aristolochia fimbriata* (Aristolochiaceae) and their contribution to gynostemium development. EvoDevo. 2020;11(4):https://doi.org/10.1186/s13227-020-00149-8.
28. Tsai W-C, Pan Z-J, Hsiao Y-Y, Jeng M-F, Wu T-F, Chen W-H, et al. Interactions of B-class complex proteins involved in tepal development in *Phalaenopsis* orchid. Plant Cell Physiol. 2008;49(5):814-24.
29. Pan ZJ, Chen YY, Du JS, Chen YY, Chung MC, Tsai WC, et al. Flower development of *Phalaenopsis* orchid involves functionally divergent *SEPALLATA*-like genes. New Phytol. 2014;202(3):1024-42.
30. Acri-Nunes-Miranda R, Mondragón Palomino M. Expression of paralogous *SEP*-, *FUL*-, *AG*- and *STK*-like MADS-box genes in wild-type and peloric *Phalaenopsis* flowers. Front Plant Sci. 2014;5(76):doi: 10.3389/fpls.2014.00076.
31. Hsu H-F, Hsu W-H, Lee Y-I, Mao W-T, Yang J-Y, Li J-Y, et al. Model for perianth formation in orchids. Nature Plants. 2015;1(5):15046;doi.org/10.1038/nplants.2015.46.
32. Huang J-Z, Lin C-P, Cheng T-C, Huang Y-W, Tsai Y-J, Cheng S-Y, et al. The genome and transcriptome of *Phalaenopsis* yield insights into floral organ development and flowering regulation. PeerJ. 2016;4:e2017.
33. Dirks-Mulder A, Butôt R, van Schaik P, Wijnands JWP, van den Berg R, Krol L, et al. Exploring the evolutionary origin of floral organs of *Erycina pusilla*, an emerging orchid model system. BMC Evol Biol. 2017;17(1):89.

34. Pramanik D, Dorst N, Meesters N, Spaans M, Smets E, Welten M, et al. Evolution and development of three highly specialized floral organs of bee pollinated *Phalaenopsis* species. EvoDevo. In review.
35. Monteiro MM, Demarco D. Corona development and floral nectaries of Asclepiadeae (Asclepiadoideae, Apocynaceae). Acta Bot Brasilica. 2017;31(3):420-32.
36. Prakash I, Singh V. Floral organogenesis in *Calotropis procera* R. Br. (Asclepiadaceae). Proc Indian natn Sci Acad B. 1993;59:79-86.
37. Puri V, Shiam R. Studies in Floral Anatomy. VIII. Vascular anatomy of the flower of certain species of the Asclepiadaceae with special reference to corona. Agra Univ J Res. 1966;15:189-216.
38. Tepfer SS. Floral anatomy and ontogeny in *Aquilegia formosa* var. *truncata* and *Ranunculus repens*. Uni Calif Pupl Bot. 1953;25:513-648.
39. Sporne KR. Some aspects of floral vascular systems. Proc Linn Soc London B. 1958;169:75-84.
40. Kunze H. Corona and nectar system in Asclepiadinae (Asclepiadaceae). Flora. 1997;192(2):175-83.
41. Theißen G, Melzer R, Rümpler F. MADS-domain transcription factors and the floral quartet model of flower development: linking plant development and evolution. Development. 2016;143(18):3259-71.
42. Suárez-Baron H, Pérez-Mesa P, Ambrose BA, González F, Pabón-Mora N. Deep into the *Aristolochia* flower: expression of C, D, and E-class genes in *Aristolochia fimbriata* (Aristolochiaceae). J Exp Zool B Mol Dev Evol. 2017;328:55-71.
43. de Oliveira RR, Cesarino I, Mazzafera P, Dornelas MC. Flower development in *Coffea arabica* L.: new insights into MADS-box genes. Plant Reprod. 2014;27(2):79-94.
44. Chase MW, Christenhusz M, Fay M, Byng J, Judd WS, Soltis D, et al. An update of the Angiosperm Phylogeny Group classification for the orders and families of flowering plants: APG IV. Bot J Linn Soc. 2016;181(1):1-20.
45. Bolger AM, Lohse M, Usadel B. Trimmomatic: a flexible trimmer for Illumina sequence data. Bioinformatics. 2014;30(15):2114-20.
46. Grabherr MG, Haas BJ, Yassour M, Levin JZ, Thompson DA, Amit I, et al. Full-length transcriptome assembly from RNA-Seq data without a reference genome. Nat Biotechnol. 2011;29(7):644.
47. Langmead B, Salzberg SL. Fast gapped-read alignment with Bowtie 2. Nature methods. 2012;9(4):357-9.
48. Li W, Godzik A. Cd-hit: a fast program for clustering and comparing large sets of protein or nucleotide sequences. Bioinformatics. 2006;22(13):1658-9.
49. Li B, Dewey CN. RSEM: accurate transcript quantification from RNA-Seq data with or without a reference genome. BMC Bioinformatics. 2011;12(1):323. https://doi.org/10.1186/471-2105-12-323.
50. Guindon S, Dufayard J-F, Lefort V, Anisimova M, Hordijk W, Gascuel O. New algorithms and methods to estimate maximum-likelihood phylogenies: assessing the performance of PhyML 3.0. Syst Biol. 2010;59(3):307-21.

Figures

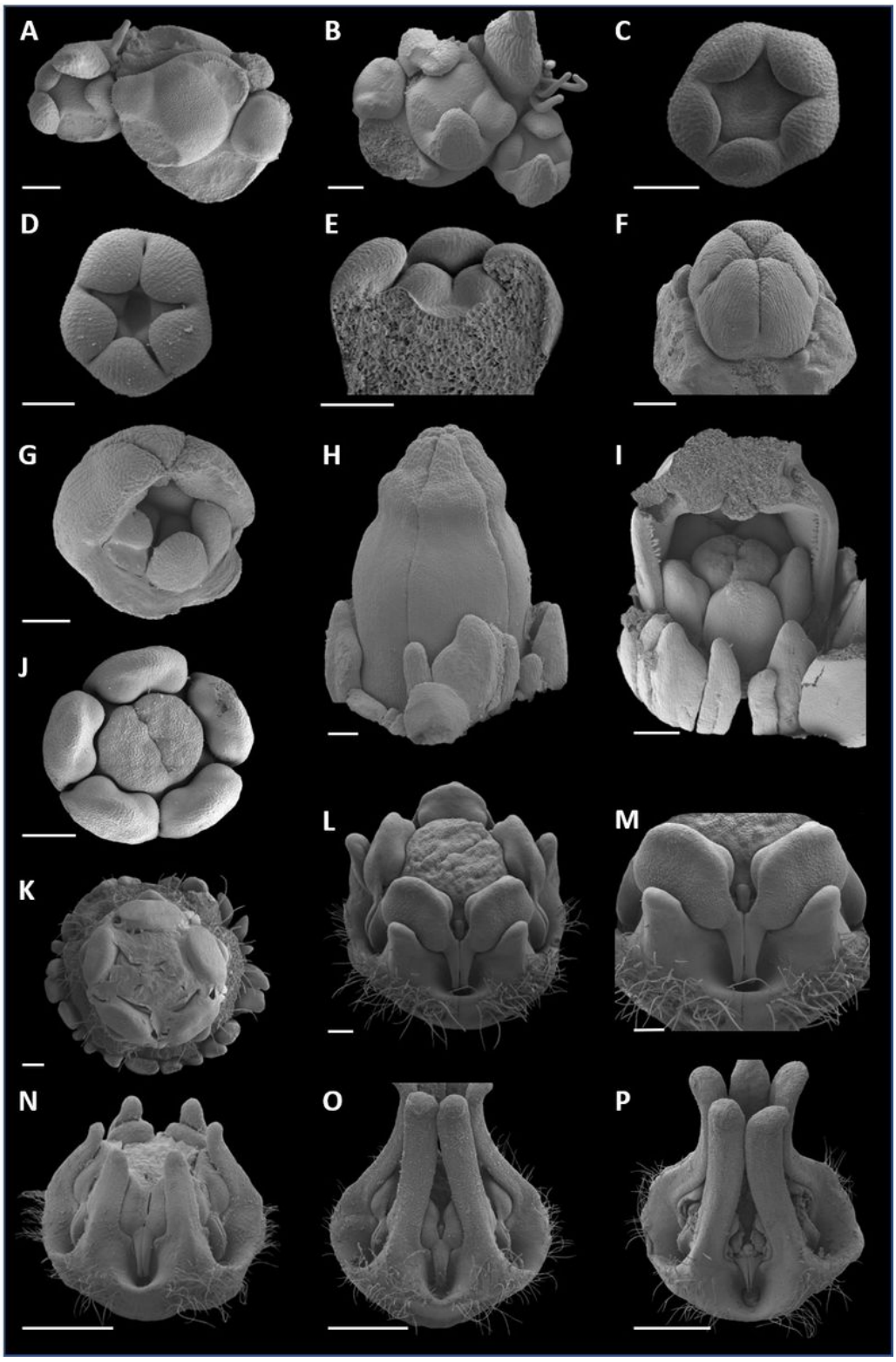

Figure 1

Ten different developmental phases (P) of Ceropegia sandersonii flowers from initiation to synorganization of floral organs. A: Shoot apex with three floral primordia, one thereof in developmental level P1. B: Shoot apex with three floral primordia with initiating sepals (P2). C: Early bud with initiated petals (P3). D: Early bud with initiated stamens (P4). E: Cross section of early bud in P4. F: Petals fully enclosing the style head (P5). G: Bud in P5 with two petals removed. H: Cylindrical corolla formed by

postgenitally fused petal tips (P6). I: Two petals removed to show gynostegium in P6. Motile trichomes visible on edges of petal tips. J: Top view of gynostegium in P6. K: Top view of gynostegium in P7 with distinct guide rails and initiating corona. L and M: Top and side view of gynostegium between P7 and P8 with distinct corpuscula. N: Side view of gynostegium in P8 with fusion between stamens and corona. Corona lobe tips outgrow the stamens. O: Side view of gynostegium in P9. P: Side view of fully developed gynostegium (P10). Scale bars: A-H + N-P: 100µm; I-M: 200µm. Images by AH.

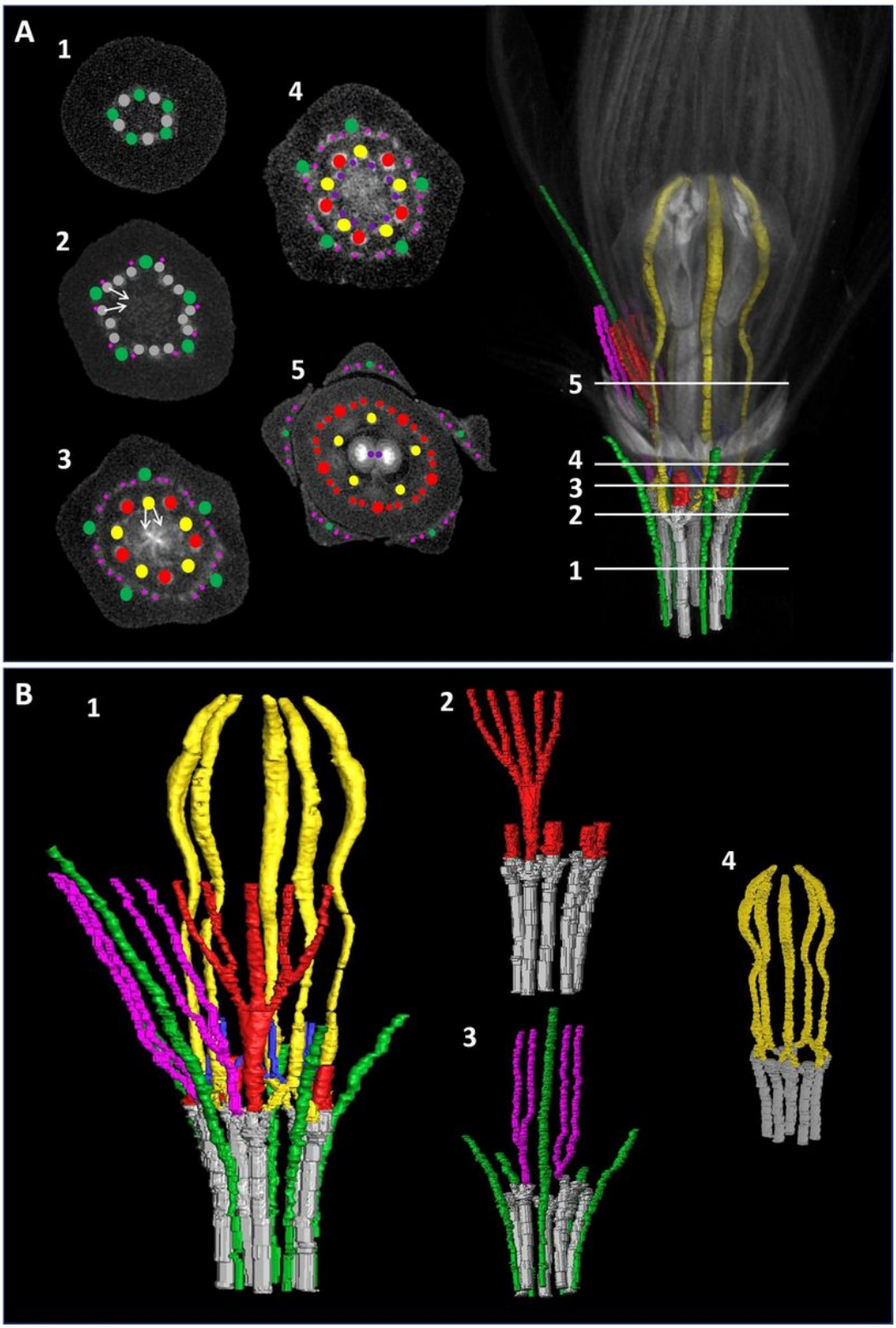

Figure 2

Reconstruction of vascular bundles in mature Ceropegia sandersonii flowers based on 3D X-ray micro-CT scanning. A: 3D scan of flower base showing cross sections (1-5) positioned where major changes in vascularization occur. Arrows in 2 and 3 indicate merging and splitting events respectively. B: Full 3D model of vascular bundles (1), and partial 3D models of petal bundles (2), sepal bundles (3), and stamen bundles (4). Colors refer to tissue specific vascular bundles as follows: grey: pedicel, green: sepals (main bundles), pink: sepals (secondary bundles), red: petals, yellow: stamens, purple: carpels. See also: 3D Movie (Additional file 7).

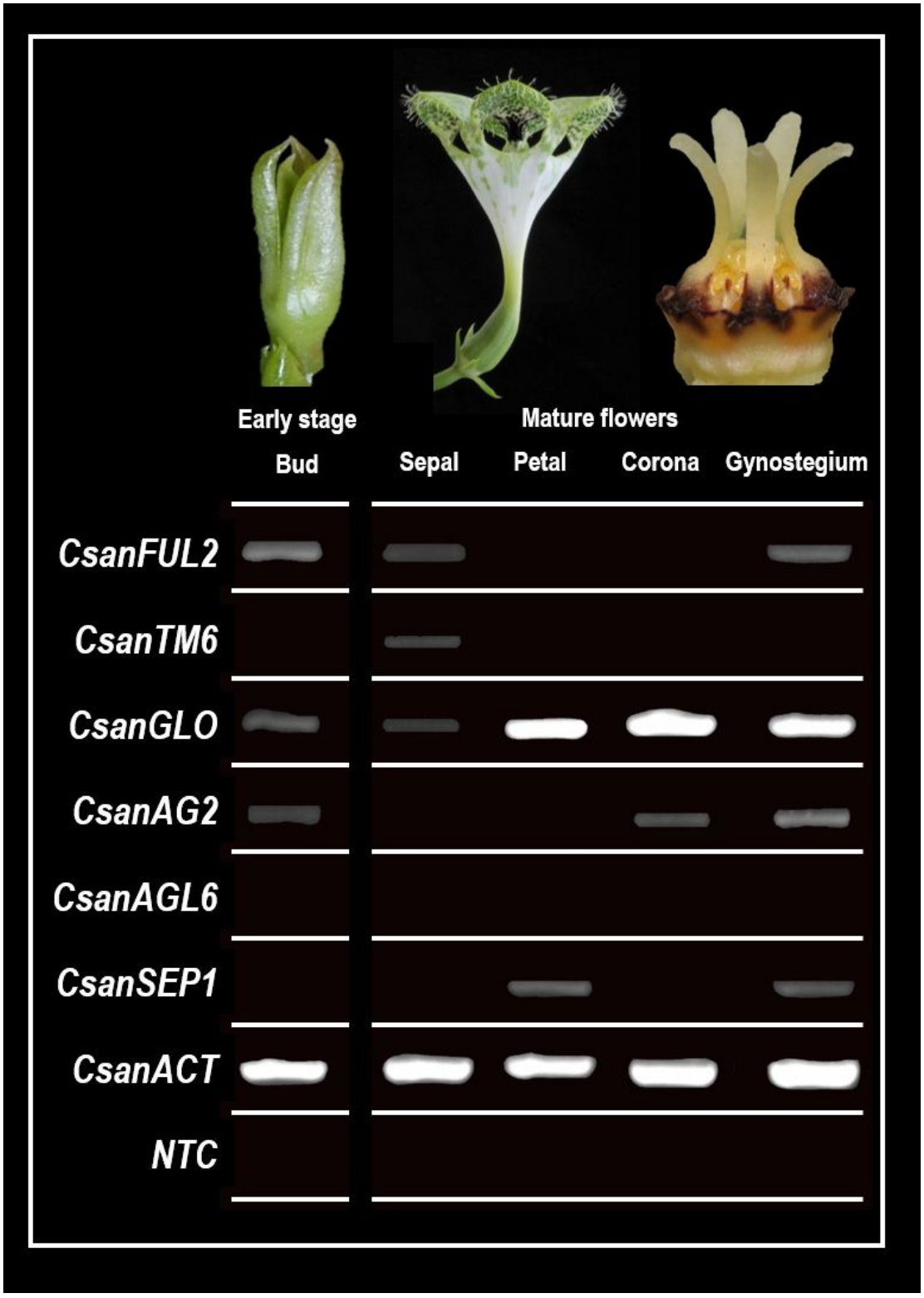

Figure 3

Expression profiles of Ceropegia sandersonii MADS-box gene homologues CsanFUL2, CsanTM6, CsanGLO, CsanSEP1, CsanAG2, CsanAGL6 in early floral buds, mature sepals, petals, corona and gynostegium. Result is based on three RT-PCR replicates per gene and tissue type. Ubiquitously expressed ACTIN (CsanACT) was used as a positive control. NTC = no template control. Photographs by AH and David Styles.

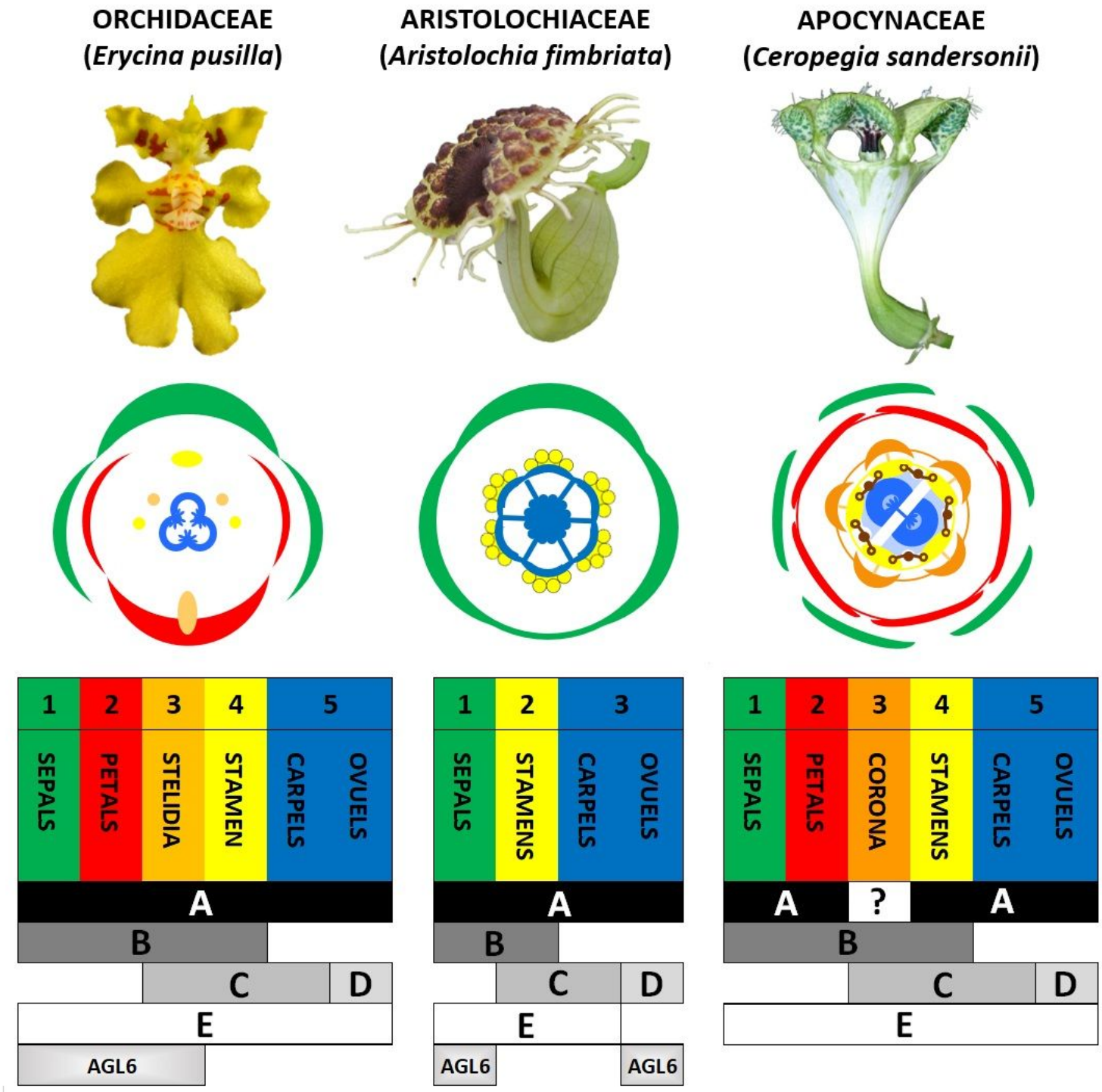

Figure 4

Models for expression of MADS-box genes involved in the differentiation of selected organs of deceptive flowers in three unrelated plant lineages. Left: orchid flowers (Orchidaceae, Erycina pusilla; based on (33). Middle: pipevine flowers (Aristolochiaceae, Aristolochia fimbriata; based on (26). Right: parachute flowers (Apocynaceae-Asclepiadoideae, Ceropegia sandersonii; this study).

Supplementary Files

This is a list of supplementary files associated with this preprint. Click to download.

- Additionalfile3.xlsx
- Additionalfile7.mpg
- Additionalfile5.png
- Additionalfile6.tif
- Additionalfile1.xlsx
- Additionalfile2.docx
- Additionalfile4.xlsx